Effects of Chloride and Ionic Strength on Physical Morphology, Dissolution, and Bacterial Toxicity of Silver Nanoparticles

ARTICLE *in* ENVIRONMENTAL SCIENCE & TECHNOLOGY · DECEMBER 2013

Impact Factor: 5.33 · DOI: 10.1021/es403969x · Source: PubMed

7 AUTHORS, INCLUDING:

Sungwoo Bae
National University of Singapore
14 PUBLICATIONS **239** CITATIONS
SEE PROFILE

Nirupam Aich
University at Buffalo, The State University of …
24 PUBLICATIONS **85** CITATIONS
SEE PROFILE

Lynn Katz
University of Texas at Austin
68 PUBLICATIONS **878** CITATIONS
SEE PROFILE

Navid B Saleh
University of Texas at Austin
68 PUBLICATIONS **3,241** CITATIONS
SEE PROFILE

Environmental Science & Technology

Article

pubs.acs.org/est

Effects of Chloride and Ionic Strength on Physical Morphology, Dissolution, and Bacterial Toxicity of Silver Nanoparticles

Bryant A. Chambers,[†] A. R. M. Nabiul Afrooz,[‡,§] Sungwoo Bae,[†] Nirupam Aich,[‡] Lynn Katz,[†] Navid B. Saleh,[‡] and Mary Jo Kirisits*[,†]

[†]Department of Civil, Architectural, and Environmental Engineering, University of Texas at Austin, Austin, Texas 78712, United States

[‡]Department of Civil and Environmental Engineering, University of South Carolina, Columbia, South Carolina 29208, United States

Supporting Information

ABSTRACT: In this study, we comprehensively evaluate chloride- and ionic-strength-mediated changes in the physical morphology, dissolution, and bacterial toxicity of silver nanoparticles (AgNPs), which are one of the most-used nanomaterials. The findings isolate the impact of ionic strength from that of chloride concentration. As ionic strength increases, AgNP aggregation likewise increases (such that the hydrodynamic radius [HR] increases), fractal dimension (D_f) strongly decreases (providing increased available surface relative to suspensions with higher D_f), and the release of $Ag_{(aq)}$ increases. With increased Ag^+ in solution, *Escherichia coli* demonstrates reduced tolerance to AgNP exposure (i.e., toxicity increases) under higher ionic strength conditions. As chloride concentration increases, aggregates are formed (HR increases) but are dominated by $AgCl^0_{(s)}$ bridging of AgNPs; relatedly, D_f increases. Furthermore, AgNP dissolution strongly increases under increased chloride conditions, but the dominant, theoretical, equilibrium aqueous silver species shift to negatively charged $AgCl_x^{(x-1)-}$ species, which appear to be less toxic to *E. coli*. Thus, *E. coli* demonstrates increased tolerance to AgNP exposure under higher chloride conditions (i.e., toxicity decreases). Expression measurements of *katE*, a gene involved in catalase production to alleviate oxidative stress, support oxidative stress in *E. coli* as a result of Ag^+ exposure. Overall, our work indicates that the environmental impacts of AgNPs must be evaluated under relevant water chemistry conditions.

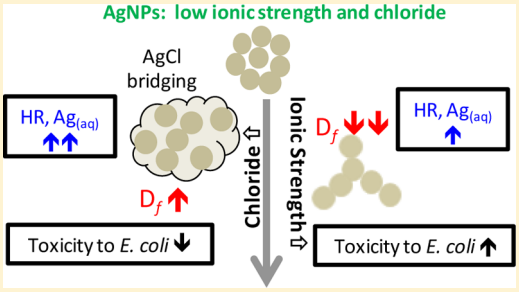

INTRODUCTION

Silver nanoparticles (AgNPs) are increasingly employed in consumer products (e.g., food storage bins and socks,[1] catheters,[2] and bandages[3]) because of their antimicrobial effects.[4−6] Increased AgNP usage translates to increased potential for their release to the environment.[7] AgNPs can exhibit toxicity to bacteria, and the mechanism of toxicity has been suggested to be based primarily on the aqueous free silver (Ag^+) produced from AgNP dissolution.[8−12] Furthermore, current research suggests that localized interfacial interaction between AgNPs and bacteria might be an important delivery mechanism of aqueous silver ($Ag_{(aq)}$) to bacteria.[4,6] Background chemistry can play a key role in modulating such interfacial interactions.

Evaluations of AgNP toxicity to bacteria abound, but the media in which bacteria are exposed to AgNPs (hereafter called "exposure solutions") vary widely. For instance, in a survey of several AgNP toxicity studies,[6,10,11,13−21] ionic strength values ranged from 0.055 mM to as high as 171 mM, and chloride concentrations from 0 mM to as high as 171 mM (Supporting Information (SI) Table S1). However, as described below, the aqueous environment affects the stability of AgNPs, a factor that is tightly connected to toxicity.[22−24]

Water chemistry strongly impacts the physical and chemical characteristics of AgNPs;[7,12,22,25−29] changes in water chemistry have been found to cause aggregation, dissolution, or stabilization.[22,25−27] For instance, ions (e.g., Cl^-, SO_4^{2-}, NO_3^-, Ca^{2+}) have been found to affect AgNP aggregation,[4,22,25,27] and chloride has been linked to increased aggregation rates.[22,27] Additionally, chloride might cause the formation of $AgCl^0_{(s)}$ shells and bridging between AgNPs,[27] possibly reducing the available AgNP surface area and dramatically changing the surface characteristics. Given that physical/chemical changes occur in AgNPs due to water chemistry and that differences in physical parameters, such as size, have been linked to differences in toxicity,[11] it follows that AgNP toxicity to bacteria also will be impacted by water chemistry.

Only a few studies have directly characterized how toxicity is affected by the chemical conditions under which bacteria are exposed to AgNPs.[22,23,25,30] The toxicity of AgNPs to bacteria has been shown to be impacted by the presence of specific

Received: September 6, 2013
Revised: December 9, 2013
Accepted: December 11, 2013

dx.doi.org/10.1021/es403969x | Environ. Sci. Technol. XXXX, XXX, XXX−XXX

Table 1. Composition of Exposure Solutions

sample	high ionic strength				medium ionic strength			low ionic strength	
parameter	Hμ140	Hμ32	Hμ2.7	Hμ0	Mμ31	Mμ2.7	Mμ0	Lμ2.7	Lμ0
pH	7.4	7.4	7.4	7.4	7.4	7.4	7.4	7.4	7.4
ionic strength (mM)	152.6	154.0	154.0	153.8	40.3	40.4	40.1	8.3	8.3
chloride (mM)	139.7	31.6	2.7		30.9	2.7		2.7	
composition									
compound (mM)	Hμ140	Hμ32	Hμ2.7	Hμ0	Mμ31	Mμ2.7	Mμ0	Lμ2.7	Lμ0
NaCl	137.1	28.9			28.2				
KCl	2.7	2.7	2.7		2.7	2.7		2.7	
$NaNO_3$		107.9	137.1	138.8		28.2	30.6		2.7
$Na_2HPO_4 \bullet 7\ H_2O$	7.5	7.5	7.5	7.5	3.3	3.3	3.3	1.7	1.7
KH_2PO_4	1.5	1.5	1.5	1.5	1.0	1.0	1.0	0.7	0.7

ligands[8,20,23] and oxygen[9] in the exposure solution. Further, it is suggested that increased chloride and ionic strength enhance the release of $Ag_{(aq)}$ from AgNPs.[27] A recent study showed that AgNP dissolution was dependent on the Cl/Ag ratio, where bactericidal effects were linked to increased $Ag_{(aq)}$;[23] however, the experiments were conducted under conditions where ionic strength and chloride concentrations were changing simultaneously, such that the impact of chloride concentration was not separated from the impact of ionic strength on toxicity. Apart from the impact of chloride on AgNP dissolution, the aggregation rate of AgNPs increases with increasing chloride concentration and ionic strength.[27,31] Thus, toxicity should be dependent on the chemistry of the exposure solution (e.g., chloride concentration and ionic strength), and differences in exposure solutions among AgNP toxicity studies likely complicate data interpretation and cross-study comparisons.

To date, no studies have comprehensively isolated the impact of variation in ionic strength from that of variation in chloride concentration on AgNP toxicity to bacteria. Furthermore, although the effect of aggregate structure on AgNP dissolution was reported recently,[32] the effect of chloride—separate from the impact of ionic strength—on such structures is still unknown. The objective of the current study is to link characteristics of the exposure solution, specifically ionic strength and chloride concentration, to the tolerance of model bacterium *Escherichia coli (E. coli)* to AgNPs. Here tolerance is defined as the ability of a bacterium to survive an antimicrobial insult. Our systematic evaluation utilized three classes of ionic strength: high (~150 mM), medium (~40 mM), and low (~8 mM). Chloride concentrations were varied from 0 to 140 mM to produce a variety of dominant aqueous silver-chloride species ($AgCl_x^{(x-1)-}$). Particular chloride concentrations in this range are representative of wastewater treatment plant effluent[33] and brackish groundwater.[34,35] Light scattering techniques (dynamic and static) and microscopy were employed to obtain information about the physical attributes of the AgNPs. A viability-based tolerance assay was used to assess AgNP toxicity to *E. coli*, and a molecular analysis was used to investigate changes in expression of an oxidative stress response gene due to AgNP exposure. Thus, this systematic evaluation of chloride- and ionic-strength-mediated physical/chemical changes in AgNPs and their impact on bacterial toxicity will be valuable in expanding our knowledge of the effect of water chemistry on the behavior of AgNPs.

MATERIALS AND METHODS

AgNP Synthesis. Mercaptosuccinic-acid-(MSA-)capped AgNPs were synthesized by sodium borohydride reduction of silver nitrate, following the procedure in Chen and Kimura (1999).[36] Much like the capping agent citrate, MSA likely exists as carboxylate groups at the nanoparticle surface at near-neutral pH. The protocol is summarized in the SI.

Bacterial Growth Conditions. A culture of *E. coli* MG4, a K-12 strain,[37] was grown in Minimal Davis (MD) medium (700 mg/L KH_2PO_4, 200 mg/L K_2HPO_4, 500 mg/L sodium citrate, 100 mg/L $MgSO_4$, 1 g/L $(NH_4)_2SO_4$, and 1 g/L glucose, pH 7.2) at 30 °C to ~10^{12} colony forming units (CFU)/mL and was inoculated to a 200-mL chemostat operated with MD medium at room temperature. Chemicals were obtained from Sigma-Aldrich and were ACS grade or higher. The chemostat was operated for at least 2 days before cells were removed for tolerance assays.

Composition of the Exposure Solutions. The composition of the solutions in which *E. coli* was exposed to AgNPs was varied. Nine exposure solutions were designed (Table 1) to cover the range of ionic strength and chloride concentrations that have been used in the literature to test AgNP toxicity to bacteria (SI Table S1). Each exposure solution is denoted by a high, medium, or low ionic strength classification (Hμ, Mμ, and Lμ, respectively) followed by the millimolar chloride concentration (i.e., Hμ32 indicates an ionic strength of 154.0 mM and a chloride concentration of 32 mM). Hμ exposure solutions (ionic strength ~150 mM) mimic the ionic strength of phosphate-buffered saline (PBS) and some growth media used in AgNP toxicity studies (see studies listed in SI Table S1); Mμ solutions (ionic strength ~40 mM) mimic some growth media (see studies listed in SI Table S1); Lμ solutions (ionic strength ~8 mM) mimic typical freshwater. At each ionic strength, the chloride concentration was varied (0 to up to 140 mM), using $NaNO_3$ to maintain the chosen ionic strength. Although the range of chloride concentrations was selected primarily based on media used in AgNP toxicity studies, these chloride concentrations have environmental relevance. The lower chloride concentrations are consistent with wastewater treatment plant effluent (1.30−3.36 mM[33]); the higher concentrations are consistent with brackish groundwater.[34,35] $Ag_{(aq)}$ speciation in each exposure solution was simulated using Visual MINTEQ (version 3.0, John Gustafsson, KTH, Sweden).

Tolerance Studies. The tolerance of *E. coli* to AgNPs or dissolved silver (dosed as $AgNO_3$) in the exposure solutions was tested by triplicate analyses of two biological replicates.

dx.doi.org/10.1021/es403969x | Environ. Sci. Technol. XXXX, XXX, XXX−XXX

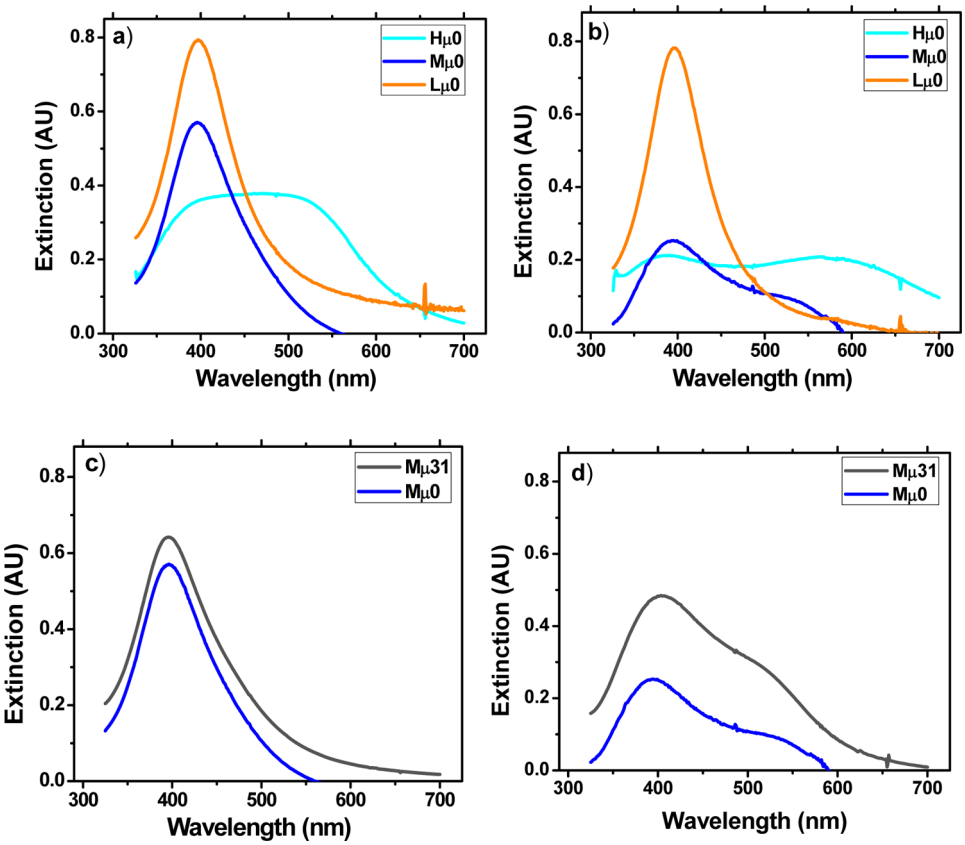

Figure 1. SPR spectra of AgNPs in selected exposure solutions. AgNPs were probed by SPR as a function of ionic strength at (a) 10 min and (b) 5 h and as a function of chloride concentration at (c) 10 min and (d) 5 h.

Planktonic cells were removed from the chemostat and washed in the appropriate exposure solution. In a 96-well microtiter plate, the exposure solution was dosed with 0−1 mg/L Ag as AgNPs or dissolved silver and inoculated to a final concentration of ~10^7 CFU/L. The plate was incubated statically for 5 h at 30 °C in the dark, and the viable cells remaining were enumerated in triplicate on Lysogeny Broth (Lennox) agar.

Quantification and Characterization of Synthesized AgNPs. To quantify AgNP concentrations, 60 μL of AgNP stock were digested in 174 μL of concentrated nitric acid (~15M) overnight and diluted with distilled deionized water (DDI). $Ag_{(aq)}$ was quantified against a silver nitrate standard (SpexCertiPrep, Metuchen, NJ) using a Varian 710 (Agilent, Santa Clara, CA) inductively coupled plasma−optical emission spectrometer (ICP-OES) with an approximate limit of detection of 5 μg/L.

The amount of $Ag_{(aq)}$ remaining in the AgNP stock after the synthesis reaction was assessed in two ways: dialyzing 1 mL of AgNP stock in pH 9 water with a 3.5-kDa molecular weight cut off (MWCO) dialysis membrane (Spectrum Laboratories, Rancho Dominguez, CA) for 14 h, changing the dialysate once after 6 h, or centrifuging the stock in an Amicon Ultra-4 centrifugal filter with a 3-kDa MWCO (Millipore, Bellerica, MA) for 40 min at 7500*g*. $Ag_{(aq)}$ in the dialysate and permeate was quantified by ICP-OES.

The size of the as-synthesized AgNPs (before suspension in an exposure solution) was characterized using transmission electron microscopy (TEM) (Tecnai Spirit, FEI, Hillsboro, OR). Samples were dropped on carbon-coated copper grids and were air-dried for 10−20 min before analysis. Images were analyzed using ImageJ (National Institutes of Health, Bethesda, MD, http://imagej.nih.gov/ij), and statistical analyses were performed in Excel (Microsoft Corp., Redmond, WA).

Characterization of AgNPs in Exposure Solutions. When added to an exposure solution, the physical/chemical AgNP characteristics were expected to change as a function of the chloride and ionic strength of the exposure solution. These changes were assessed as follows.

The production of $Ag_{(aq)}$ in the exposure solutions was assessed. AgNPs were dosed (1 mg/L) to 3.4 mL of an exposure solution and incubated statically at 30 °C in the dark. Samples were withdrawn at 10 min and 1, 3, and 5 h and processed with an Amicon Ultra-4 3-kDa centrifugal filter (7500*g* for 30 min) to separate $Ag_{(aq)}$ from AgNPs and aggregates. The permeate was acidified to a final concentration of 2% nitric acid for analysis by ICP-OES.

Surface characteristics were examined qualitatively via surface plasmon resonance (SPR) with a UV-visible spectrophotometer (Agilent 8453, Santa Clara, CA). AgNPs were dispersed (1 mg/L) in each exposure solution in a 10-cm quartz cuvette and incubated statically at 30 °C in the dark. Readings were taken at 10 min and 1, 3, and 5 h.

The size and aggregate structure of the AgNPs in the exposure solutions were assessed. Light scattering measurements were conducted on an ALV-CGS/3 goniometer system (ALV-GmbH, Langen, Germany). The size of the aggregating AgNPs was measured over time via dynamic light scattering (DLS). The DLS protocol is described in detail elsewhere[38,39] and is summarized in the SI. The mean hydrodynamic radius (HR) and standard deviation were computed over 1-h intervals (0−5 h) and are reported at the midpoint of each interval.

dx.doi.org/10.1021/es403969x | *Environ. Sci. Technol.* XXXX, XXX, XXX−XXX

Static light scattering (SLS) measurements were performed to describe the aggregate structure (i.e., fractal dimension) of the AgNPs. The SLS protocol is described in detail in Khan et al. (2013)[39] and is summarized in the SI. Changes in AgNP morphology (e.g., independent particles versus bridged particles) and elemental composition were evaluated by scanning electron microscopy (SEM) and energy dispersive X-ray (EDX) spectroscopy, respectively, and these methods are summarized in the SI. Additionally, TEM was performed on AgNPs exposed to Hμ140 using an H8000 TEM (Hitachi High Technologies, Roselyn Heights, NY). Samples were dropped on carbon/Formvar-coated copper grids and were air-dried for 15−20 min before imaging.

Reverse-Transcription, Quantitative Real-time Polymerase Chain Reaction (RT-qPCR). The expression of *katE* was studied to understand how *E. coli* responds to AgNPs in different exposure solutions. The cells were grown in batch culture in MD medium, pelleted, and washed in Lμ0. One-milliliter aliquots of washed cells were added to duplicate selected exposure solutions (Hμ0, Mμ31, and Lμ0) in the presence or absence of AgNPs at an initial cell concentration of 3×10^7 CFU/mL. Cells were incubated in the dark for 5 h with shaking at 30 °C. An aliquot from each flask was removed for cell enumeration by viable plate counts on Lysogeny Broth (Lennox) agar, and the remaining cells were pelleted for RNA isolation. RNA was extracted in duplicate from each flask and pooled, and cDNA was synthesized in duplicate reactions and pooled; detailed protocols are given in the SI.

qPCR primers targeting a 190-bp *katE* fragment were designed using Primer3 software[40] and *E. coli* K-12 substrain MG1655, which has a sequenced genome. qPCR was run on each cDNA sample in triplicate, according to the protocol in the SI. A *katE* standard curve was constructed using genomic DNA from *E. coli* MG4 (10^1−10^7 gene copies/reaction). A Student's *t* test was performed (α = 0.05) in Minitab 16 (Minitab Inc., State College, PA).

RESULTS AND DISCUSSION

Characterization of Synthesized AgNPs. After synthesis, AgNPs in pH 9 DDI were characterized. TEM analysis showed spherical particles with an exponential distribution and average diameter of 2.9 nm (SI Figure S1), in close agreement with the 2.2-nm diameter described in the original synthesis.[36] A typical batch of AgNPs contained 220 mg/L total silver, of which 7−9 μg/L was residual $Ag_{(aq)}$. When the AgNP stock was diluted for bacterial tolerance studies (≤1 mg/L), the residual $Ag_{(aq)}$ concentration was orders of magnitude below inhibitory levels.

Aggregation. We used SPR to generally assess AgNP aggregation under different ionic strength and chloride conditions (Figure 1). SPR has been used previously to qualitatively characterize AgNPs.[24,31] AgNPs typically have an extinction peak near 400 nm,[31,41] but this can shift based on the local refractive index and NP diameter.[42−44]

Figure 1a−b highlights temporal changes in the SPR spectra as a function of ionic strength at a constant chloride concentration (0 mM). At the lowest ionic strength (Lμ0), the original AgNP extinction peak intensity remained nearly constant over time, indicating AgNP stability. However, at increased ionic strengths (Mμ0 and Hμ0), a rapid decrease in the original AgNP extinction peak intensity and peak broadening occurred, which suggests the depletion of stable AgNPs and the formation of aggregates, respectively.[22] Relatedly, the DLS data show that the average HR at 5 h increased from 33.6 ± 0.7 nm for Lμ0 to 51.2 ± 1.2 nm for Hμ0 (SI Figure S2a). Thus, the aggregation behavior observed via SPR, which is a technique that probes individual nanoscale interactions, is complemented by DLS, a technique that measures average suspension properties. Figure 1c−d highlights temporal changes in the SPR spectra as a function of chloride concentration at constant ionic strength (~40 mM); the lowest and highest chloride concentrations at this ionic strength (0 and 31 mM chloride, respectively) were assessed because the changes in the SPR spectra as a function of chloride concentration were not nearly as dramatic as those as a function of ionic strength. Over time, both SPR spectra (Mμ0 and Mμ31) show reduction in the original AgNP extinction peak intensity as well as peak broadening and formation of a secondary peak at 564 nm. However, the peak intensity reduction at 390 nm is not as significant in the Mμ31 sample, suggesting less aggregation of primary AgNPs in the presence of chloride. That is, AgCl bridging between AgNPs might reduce AgNP−AgNP aggregation but cause the formation of larger overall AgNP/AgCl aggregates. This is supported by DLS, which interrogates the overall aggregate size (AgNP plus AgCl bridging), where the average HR at 5 h increased from 33.6 ± 0.7 nm for Mμ0 to 158.4 ± 70.5 nm for Mμ31 (SI Figure S2b). In contrast, SPR probes individual nanoscale interactions, and it indicates little effect of chloride on those AgNPs. A similar trend was observed in the SPR spectra for AgNPs exposed to Hμ0 and Hμ140 (data not shown), where the presence of chloride appeared to stabilize AgNPs relative to the absence of chloride. Overall, the SPR data suggest that ionic strength is a major factor in AgNP destabilization and chloride acts to stabilize AgNPs. Evidence of AgCl bridging to stabilize AgNPs is provided in the Aggregate Structure section.

Dissolution. The release of $Ag_{(aq)}$ due to the dissolution of AgNPs under different ionic strength and chloride conditions was examined (Figure 2). The release of $Ag_{(aq)}$ from AgNPs is dependent upon oxidation,[8,23] and we detected $Ag_{(aq)}$ in the exposure solutions dosed with AgNPs. In the absence of chloride, ionic strength only slightly impacted the initial release (at 10 min) of $Ag_{(aq)}$ (Figure 2 inset). However, for a constant ionic strength, the initial release of $Ag_{(aq)}$ from AgNPs was strongly affected by the presence of chloride in the exposure

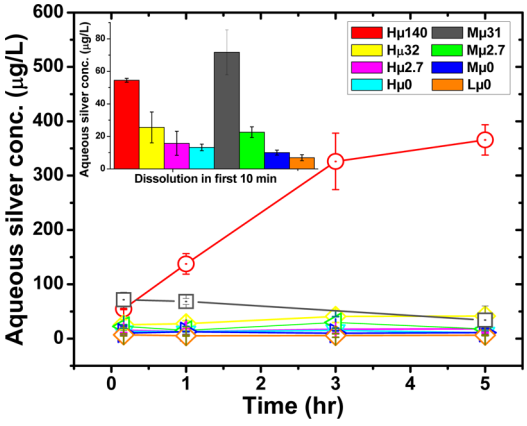

Figure 2. Dissolution of AgNPs (dosed at 1 mg/L) over time as a function of ionic strength and chloride concentration, where the inset highlights the release of $Ag_{(aq)}$ after 10 min. Data points are the average of triplicate experiments, and error bars show one standard deviation.

dx.doi.org/10.1021/es403969x | Environ. Sci. Technol. XXXX, XXX, XXX−XXX

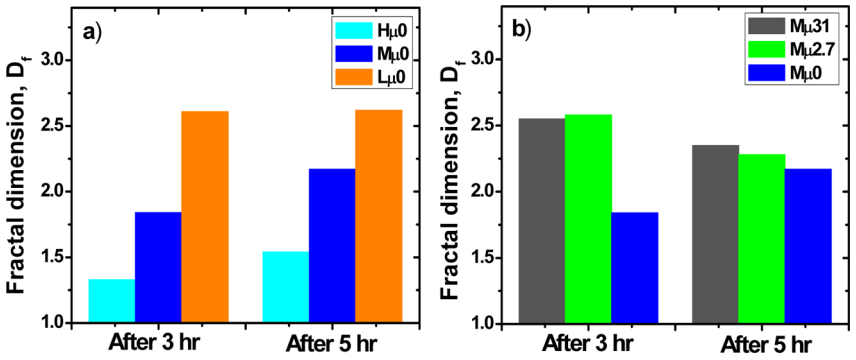

Figure 3. Fractal dimension of AgNPs as a function of (a) ionic strength and (b) chloride concentration.

solution (Figure 2 inset). These data are consistent with previous literature findings that show rapid AgNP dissolution.[23,45] We continued to monitor $Ag_{(aq)}$ over 5 h, which corresponds to the time frame of our tolerance studies, and only saw continued AgNP dissolution at the highest chloride concentration (Hμ140, Figure 2). This is consistent with previous studies that have suggested that chloride might act catalytically in the dissolution of AgNPs.[46,47] Thus, our data indicate that chloride concentration is more important than ionic strength in driving the production of $Ag_{(aq)}$ from AgNP dissolution.

Aggregate Structure. Aggregate structure formation under different ionic strength and chloride conditions was examined via SLS (Figure 3). For a constant chloride concentration (0 mM), the fractal dimension (D_f) decreased with increasing ionic strength (Figure 3a). This observation is consistent with classical electrostatic screening-induced fractal formation of colloids, as observed previously.[39] Higher ionic strength reduces the electrostatic potential, which likely imparted "stickiness" to the AgNPs and resulted in lower D_f (i.e., a more fractal structure as compared to a more densely packed aggregate in Lμ0). On the other hand, at constant ionic strength (~40 mM), increased chloride concentrations showed increased D_f (Figure 3b). This shift in structure toward a more compact form in the presence of chloride supports the bridging of AgNPs via silver chloride ($AgCl^0_{(s)}$) formation. Using TEM, a similar observation of $AgCl^0_{(s)}$-induced bridging of AgNPs has been observed previously.[45]

While light-scattering techniques were used to assess aggregate size and structure, SEM was used to provide visual evidence of morphological changes under different water chemistry conditions. SEM provides support for AgNP bridging in the presence of high chloride concentrations, as shown for AgNPs in Hμ140 (SI Figure S3c,d) as compared to AgNPs in Mμ31 and Hμ0 (SI Figure S3a,b). Furthermore, TEM of AgNPs in Hμ140 shows a change in contrast at the particle−particle attachment regions (indicated by arrows in SI Figure S3e), which is indicative of bridging through chloride precipitation. EDX confirms the presence of Ag in the pristine AgNPs (SI Figure S4a); Na and Si peaks in the spectrum are likely due to the glass slide used for SEM, as these peaks appear in the spectra for all tested exposure solutions. EDX also confirms the presence of Ag and Cl on the aggregated particle clusters in Mμ31 and Hμ140, further supporting the reaction of chloride on AgNP surfaces (SI Figure S4b,c).

Impact of Ionic Strength and Chloride on Bacterial Tolerance to AgNPs. As demonstrated above, the chemistry of the exposure solution impacts AgNP stability. Next we examined the tolerance of *E. coli* to AgNPs in the nine exposure solutions; selected results are shown herein.

Figure 4 demonstrates the tolerance of *E. coli* to AgNPs as a function of ionic strength at a constant chloride concentration

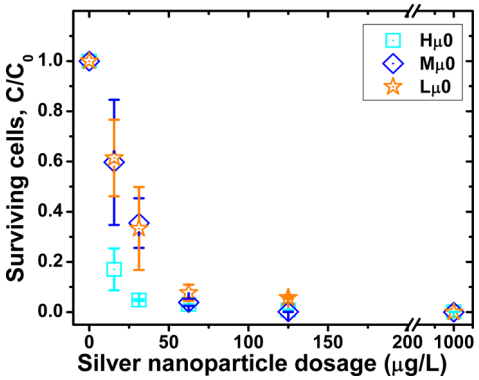

Figure 4. Impact of ionic strength on the tolerance of *E. coli* to AgNPs. Surviving cells are shown as a function of AgNP dose. Data are averages of triplicate assays of biological duplicates, and error bars represent one standard deviation.

(0 mM). At higher AgNP concentrations (greater than 50 μg/L), *E. coli* survival is less than 10%. At lower AgNP concentrations (15.6 and 31.2 μg/L), *E. coli* has the lowest tolerance to AgNPs under the highest ionic strength condition (Hμ0). This is likely due to one or more of the following reasons. (1) Hμ0 induces higher AgNP dissolution as compared to lower ionic strength exposure solutions (e.g., 15.3 and 5.6 μg/L $Ag_{(aq)}$ measured in the bulk solution after a 3-h exposure of AgNPs to Hμ0 and Lμ0, respectively, Figure 2), and Ag^+ is biocidal to bacteria.[8,48,49] (2) Hμ0 causes the most compression of the electric double layer, which would facilitate closer proximity of cells to AgNPs. (3) Hμ0 induces a different aggregate structure as compared to lower ionic strengths. At higher ionic strengths, AgNPs were found to form more fractal structures (lower D_f) as compared to more densely packed structures at lower ionic strengths (Figure 3a), which leads to more available surface area for interaction with bacteria. Close interaction of bacteria with AgNPs could facilitate the delivery of Ag^+ to the cells as the AgNPs dissolve, resulting in reduced tolerance of *E. coli* to AgNPs at higher ionic strengths.

Figure 5a demonstrates the tolerance of *E. coli* to AgNP exposure as a function of chloride concentration at constant ionic strength (~40 mM). *E. coli* has the highest tolerance to AgNPs under the highest chloride condition shown (Mμ31).

dx.doi.org/10.1021/es403969x | Environ. Sci. Technol. XXXX, XXX, XXX−XXX

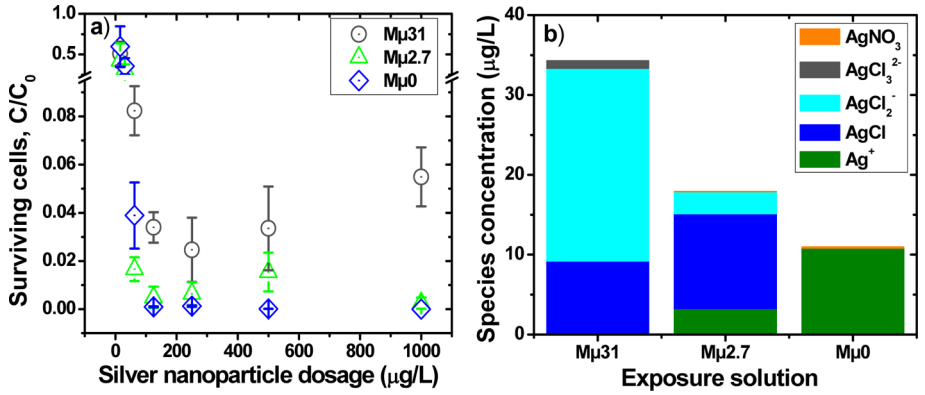

Figure 5. Impact of chloride on tolerance of *E. coli* to AgNPs. (a) Surviving cells as a function of AgNP dose; (b) theoretical equilibrium $AgCl_x^{(x-1)-}$ speciation of $Ag_{(aq)}$ produced 5 h after 1 mg/L AgNPs are dosed to a particular exposure solution, where $Ag_{(aq)}$ for each exposure solution is shown in Figure 2. Cell data are the averages of triplicate assays of biological duplicates, and error bars represent one standard deviation.

This is likely due to one or both of the following reasons. (1) Higher chloride concentrations result in more AgNP dissolution (Figure 2), but they produce lower concentrations of Ag^+ and the neutral species $AgCl^0_{(aq)}$ (compare Mμ31 to Mμ2.7 in Figure 5b). While some work has proposed that only the total concentration of aqueous $AgCl_x^{(x-1)-}$ species, rather than their speciation, controls the overall toxicity to *E. coli*, [23] our work makes the claim that $AgCl_x^{(x-1)-}$ speciation matters. As shown in SI Figure S5 (where aqueous silver was dosed to *E. coli*), the tolerance of *E. coli* to $Ag_{(aq)}$ increases as the charge on the dominant $AgCl_x^{(x-1)-}$ species decreases (e.g., greater tolerance when $AgCl_2^-$ is the dominant species as compared to when Ag^+ is the dominant species). However, given the values of the $AgCl_x^{(x-1)-}$ stability constants, it is not possible to isolate the toxicity impact of each $AgCl_x^{(x-1)-}$ species. (2) Chloride induces changes in AgNP aggregate structure. When chloride is low or absent (Mμ2.7 and Mμ0, respectively), AgNPs form more fractal structures (Figure 3b). This leads to higher available surface area for interaction with bacteria, likely facilitating the delivery of $Ag_{(aq)}$ to the cells as the AgNPs dissolve, resulting in reduced tolerance of *E. coli* to AgNPs at lower chloride concentrations. Our results are in contrast with an earlier study[23] that showed reduced tolerance of *E. coli* to AgNPs in the presence of higher chloride concentrations, but those results are likely confounded by simultaneous changes in ionic strength and chloride concentration.

Oxidative Stress in *E. coli* Due to AgNP Exposure. To further assess the effect of AgNPs on *E. coli* under different ionic strength and chloride conditions, we analyzed the expression of a gene linked to oxidative stress, *katE*.[50,51] *katE* encodes a component of the catalase hydroperoxidase II and is responsible for alleviating the effects of oxidative stress and also is linked to chromate resistance.[51,52] Catalase hydroperoxidase II converts hydrogen peroxide to molecular oxygen and water and limits the transition-metal-facilitated formation of hydroxyl radicals via a Fenton-type reaction.[50] While the extent to which AgNP toxicity is linked to reactive oxygen species (ROS) formation is still debated,[8,12,53,54] Ag^+ toxicity has been linked to ROS formation;[55] furthermore, this study (Figure 5b) corroborates previous findings[9,11,12] that AgNP toxicity is linked to Ag^+ (though other $AgCl_x^{(x-1)-}$ species also might contribute to toxicity). We examined the expression of *katE* in the presence of a low concentration of AgNPs (20 μg/L), which killed only a fraction of the exposed population (Figures 4 and 5a).

The expression of *katE* under the tested conditions is shown in Figure 6. *katE* expression increased significantly (p-value = 0.001) in Hμ0 in the presence of AgNPs (Hμ0-AgNP) as compared to the control (absence of AgNPs, Hμ0-Ctrl). By comparison, *katE* expression did not increase significantly (p-value = 0.194) in Lμ0 in the presence of AgNPs (Lμ0-AgNP) as compared to its control (Lμ0-Ctrl). This is consistent with the AgNP dissolution data, which showed greater $Ag_{(aq)}$ in the bulk solution when AgNPs were dosed to Hμ0 as compared to Lμ0 (Figure 2 inset). Relatedly, *katE* expression did not increase significantly (p-value = 0.077) in Mμ31 in the presence of AgNPs (Mμ31-AgNP) as compared to its control (Mμ31-Ctrl). This is consistent with theoretical equilibrium speciation for $AgCl_x^{(x-1)-}$, which indicates that Ag^+ in the Mμ31 bulk solution is inconsequential (Figure 5b). Overall, these data support oxidative stress in *E. coli* as a result of Ag^+ exposure.

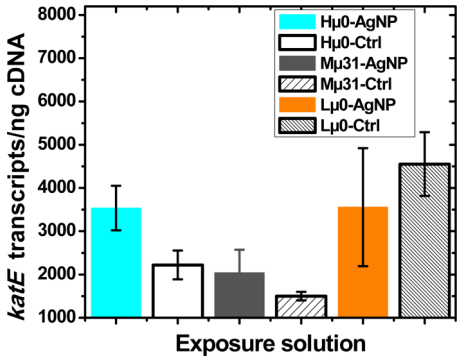

Figure 6. *katE* expression in *E. coli* as a function of AgNP exposure under different ionic strength and chloride conditions. Gene expression was measured in three exposure solutions (Hμ0, Mμ31, and Lμ0) in the presence of AgNPs and the absence of AgNPs (controls). Data are averages of triplicate qPCR reactions from duplicate biological experiments. Error bars represent one standard deviation.

Mechanism of Toxicity. The key mechanism underlying the observed antimicrobial activity of AgNPs in this study is the role of background electrolytes in altering AgNP physical/chemical properties. Both ionic strength and chloride concentration affect the physical morphology, dissolution, and bacterial toxicity of AgNPs (Figure 7). As ionic strength increases, AgNP aggregation likewise increases (such that the HR increases), D_f strongly decreases (providing increased

dx.doi.org/10.1021/es403969x | Environ. Sci. Technol. XXXX, XXX, XXX−XXX

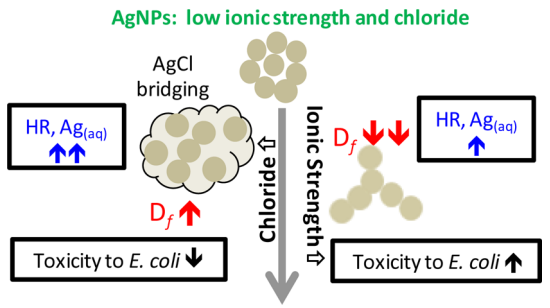

Figure 7. Model of the effects of chloride and ionic strength on physical morphology, dissolution, and bacterial toxicity of AgNPs.

available surface relative to suspensions with higher D_f), the release of $Ag_{(aq)}$ increases, and *E. coli* demonstrates reduced tolerance to the AgNP exposure (i.e., toxicity increases). As chloride concentration increases, aggregates are formed but are dominated by $AgCl^0_{(s)}$ bridging of AgNPs; relatedly, the fractal dimension increases. Furthermore, AgNP dissolution is strongly increased under increased chloride conditions, but the dominant aqueous silver species shift to negatively charged $AgCl_x^{(x-1)-}$ species, which appear to be less toxic to *E. coli* (SI Figure S5). Thus, *E. coli* demonstrates increased tolerance to the AgNP exposure under higher chloride conditions (i.e., toxicity decreases).

Previous work on the antimicrobial activity of AgNPs reports the complexity in assessing dissolution of AgNPs in the presence of chloride ions.[23] Our study is the first to postulate the correlation of observed toxicity of AgNPs with their dissolution and physical characteristics (i.e., aggregation, fractal structure, particle bridging) for a wide range of chemical conditions. Moreover, the correlation of toxicity with $Ag_{(aq)}$ speciation and the use of gene expression analysis to examine the role of ROS in the observed toxicity of AgNPs are important components of our mechanistic analysis. Furthermore, the findings in this study allow us to draw new conclusions about the impact of chloride, separate from the impact of ionic strength, on the dissolution, physical characteristics, and toxicity of AgNPs.

Environmental Implications. With respect to bacterial toxicity testing for AgNPs, it is important to recognize that dramatic changes in physical morphology and dissolution can occur as a result of the chosen water chemistry conditions. Toxicity testing often occurs under conditions of elevated ionic strength and chloride, but this will not typically reflect relevant environmental conditions where bacteria might be exposed to AgNPs (e.g., in wastewater treatment). In the case of *E. coli*, it is likely that the increased AgNP toxicity due to high ionic strength conditions would just balance the decreased AgNP toxicity due to high chloride conditions (Figure 7), but this fortuitous occurrence might not be true for all microorganisms. Thus, toxicity assessments of NPs to microorganisms should be conducted under environmentally relevant water chemistry conditions. Furthermore, the environmental impacts of AgNPs must consider dissolution, speciation, and aggregation for the particular water chemistry of interest. For instance, environmental conditions influencing AgNP physical properties might influence the manifestation of the AgNP chemical behavior (e.g., fractal-structure-dependent dissolution), which can then affect toxicity.

■ ASSOCIATED CONTENT

Supporting Information

Detailed information regarding methods and additional results. This material is available free of charge via the Internet at http://pubs.acs.org.

■ AUTHOR INFORMATION

Corresponding Author

*Phone: (512) 232-7120; fax: (512) 471-0592; e-mail: kirisits@utexas.edu.

Present Address

[§]Department of Civil, Architectural, and Environmental Engineering, University of Texas at Austin, Austin, Texas 78712, United States.

Notes

The authors declare no competing financial interest.

■ ACKNOWLEDGMENTS

We thank the National Science Foundation (CBET 0846719 to M.J. Kirisits) for funding and the following people for technical assistance: Taegyu Kim (tolerance assays), Colleen Lyons (TEM), and Gustavo Ochoa and Katie Speights (laboratory support). We also thank Dr. Soumitra Ghoshroy and Erika Balogh at the University of South Carolina Electron Microscopy Center for assistance with TEM and SEM.

■ REFERENCES

(1) Fauss, E. *Silver Nanotechnology Commercial Inventory*; The Project for Emerging Nanotechnologies, 2008. http://www.nanotechproject.org.

(2) Roe, D.; Karandikar, B.; Bonn-Savage, N.; Gibbins, B.; Roullet, J. B. Antimicrobial surface functionalization of plastic catheters by silver nanoparticles. *J. Antimicrob. Chemother.* **2008**, *61* (4), 869−876, DOI: 10.1093/jac/dkn034.

(3) Lee, H. Y.; Park, H. K.; Lee, Y. M.; Kim, K.; Park, S. B. A practical procedure for producing silver nanocoated fabric and its antibacterial evaluation for biomedical applications. *Chem. Commun.* **2007**, *28*, 2959−2961, DOI: 10.1039/B703034G.

(4) Levard, C.; Hotze, E. M.; Lowry, G. V.; Brown, G. E. Environmental transformations of silver nanoparticles: Impact on stability and toxicity. *Environ. Sci. Technol.* **2012**, *46* (13), 6900−6914, DOI: 10.1021/es2037405.

(5) Luoma, S. N. *Silver Nanotechnologies and the Environment: Old Problems or New Challenges?*; Woodrow Wilson International Center for Scholars: Washington, DC, 2008.

(6) Morones, J. R.; Elechiguerra, J. L.; Camacho, A.; Holt, K.; Kouri, J. B.; Ramírez, J. T.; Yacaman, M. J. The bactericidal effect of silver nanoparticles. *Nanotechnology* **2005**, *16* (10), 2346−2353, DOI: 10.1088/0957-4484/16/10/059.

(7) Nowack, B.; Bucheli, T. D. Occurrence, behavior and effects of nanoparticles in the environment. *Environ. Pollut.* **2007**, *150* (1), 5−22, DOI: 10.1016/j.envpol.2007.06.006.

(8) Xiu, Z. M.; Ma, J.; Alvarez, P. J. J. Differential effect of common ligands and molecular oxygen on antimicrobial activity of silver nanoparticles versus silver ions. *Environ. Sci. Technol.* **2011**, *45* (20), 9003−9008, DOI: 10.1021/es201918f.

(9) Xiu, Z. M.; Zhang, Q. B.; Puppala, H. L.; Colvin, V. L.; Alvarez, P. J. J. Negligible particle-specific antibacterial activity of silver nanoparticles. *Nano Lett.* **2012**, *12* (8), 4271−4275, DOI: 10.1021/nl301934w.

(10) Bae, E.; Park, H. J.; Lee, J.; Kim, Y.; Yoon, J.; Park, K.; Choi, K.; Yi, J. Bacterial cytotoxicity of the silver nanoparticle related to physicochemical metrics and agglomeration properties. *Environ. Toxicol. Chem.* **2010**, *29* (10), 2154−2160, DOI: 10.1002/etc.278.

(11) Sotiriou, G. A.; Pratsinis, S. E. Antibacterial activity of nanosilver ions and particles. *Environ. Sci. Technol.* **2010**, *44* (14), 5649−5654, DOI: 10.1021/es101072s.
(12) Arnaout, C. L.; Gunsch, C. K. Impacts of silver nanoparticle coating on the nitrification potential of *Nitrosomonas europaea*. *Environ. Sci. Technol.* **2012**, *46* (10), 5387−5395, DOI: 10.1021/es204540z.
(13) Barani, H.; Montazer, M.; Samadi, N.; Toliyat, T. Nano silver entrapped in phospholipids membrane: Synthesis, characteristics and antibacterial kinetics. *Mol. Membr. Biol.* **2011**, *28* (4), 206−215, DOI: 10.3109/09687688.2011.565484.
(14) Choi, O. K.; Hu, Z. Q. Nitrification inhibition by silver nanoparticles. *Water Sci. Technol.* **2009**, *59* (9), 1699−1702, DOI: 10.2166/wst.2009.205.
(15) Sondi, I.; Salopek-Sondi, B. Silver nanoparticles as antimicrobial agent: A case study on *E. coli* as a model for gram-negative bacteria. *J. Colloid Interface Sci.* **2004**, *275* (1), 177−182, DOI: 10.1016/j.jcis.2004.02.012.
(16) Lok, C. N.; Ho, C. M.; Chen, R.; He, Q. Y.; Yu, W. Y.; Sun, H.; Tam, P. K. H.; Chiu, J. F.; Che, C. M. Proteomic analysis of the mode of antibacterial action of silver nanoparticles. *J. Proteome Res.* **2006**, *5* (4), 916−924, DOI: 10.1021/pr0504079.
(17) Kim, J. S. J. H.; Kuk, E.; Yu, K. N.; Park, S. J.; Lee, H. J.; Kim, S. H.; Park, Y. K. Y. H.; Hwang, C. Y.; Kim, Y. K.; Lee, Y. S.; Jeong, D. H.; Cho, M. H. Antimicrobial effects of silver nanoparticles. *Nanomed.: Nanotechnol., Biol. Med.* **2007**, *3* (1), 95−101, DOI: 10.1016/j.nano.2006.12.001.
(18) Choi, O.; Deng, K. K.; Kim, N. J.; Ross, L.; Surampalli, R. Y.; Hu, Z. The inhibitory effects of silver nanoparticles, silver ions, and silver chloride colloids on microbial growth. *Water Res.* **2008**, *42* (12), 3066−3074, DOI: 10.1016/j.watres.2008.02.021.
(19) Fabrega, J.; Fawcett, S. R.; Renshaw, J. C.; Lead, J. R. Silver nanoparticle impact on bacterial growth: Effect of pH, concentration, and organic matter. *Environ. Sci. Technol.* **2009**, *43* (19), 7285−7290, DOI: 10.1021/es803259g.
(20) Jin, X.; Li, M.; Wang, J.; Marambio-Jones, C.; Peng, F.; Huang, X.; Damoiseaux, R.; Hoek, E. M. V. High-throughput screening of silver nanoparticle stability and bacterial inactivation in aquatic media: Influence of specific ions. *Environ. Sci. Technol.* **2010**, *44* (19), 7321−7328, DOI: 10.1021/es100854g.
(21) Kim, S. W.; Baek, Y. W.; An, Y. J. Assay-dependent effect of silver nanoparticles to *Escherichia coli* and *Bacillus subtilis*. *Appl. Microbiol. Biotechnol.* **2011**, *92* (5), 1045−1052, DOI: 10.1007/s00253-011-3611-x.
(22) Tejamaya, M.; Römer, I.; Merrifield, R. C.; Lead, J. R. Stability of citrate, PVP, and PEG coated silver nanoparticles in ecotoxicology media. *Environ. Sci. Technol.* **2012**, *46* (13), 7011−7017, DOI: 10.1021/es2038596.
(23) Levard, C.; Mitra, S.; Yang, T.; Jew, A. D.; Badireddy, A. R.; Lowry, G. V.; Brown, G. E. Effect of chloride on the dissolution rate of silver nanoparticles and toxicity to *E. coli*. *Environ. Sci. Technol.* **2013**, *47* (11), 5738−5745, DOI: 10.1021/es400396f.
(24) Kvítek, L.; Panácek, A.; Soukupova, J.; Kolar, M.; Vecerova, R.; Prucek, R.; Holecova, M.; Zboril, R. Effect of surfactants and polymers on stability and antibacterial activity of silver nanoparticles. *J. Phys. Chemistry* **2008**, *122* (15), 5825−5834, DOI: 10.1021/jp711616v.
(25) Cumberland, S. A; Lead, J. R. Particle size distributions of silver nanoparticles at environmentally relevant conditions. *J. Chromatogr.* **2009**, *1216* (52), 9099−9105, DOI: 10.1016/j.chroma.2009.07.021.
(26) Deonarine, A.; Lau, B. L. T.; Aiken, G. R.; Ryan, J. N.; Hsu-Kim, H. Effects of humic substances on precipitation and aggregation of zinc sulfide nanoparticles. *Environ. Sci. Technol.* **2011**, *45* (8), 3217−3223, DOI: 10.1021/es1029798.
(27) Li, X.; Lenhart, J. J.; Walker, H. W. Dissolution-accompanied aggregation kinetics of silver nanoparticles. *Langmuir* **2010**, *26* (22), 16690−16698, DOI: 10.1021/la101768n.
(28) Aiken, G.; Hsu-Kim, H.; Ryan, J. Influence of dissolved organic matter on the environmental fate of metals, nanoparticles, and colloids. *Environ. Sci. Technol.* **2011**, *45* (8), 3196−3201, DOI: 10.1021/es103992s.
(29) Wigginton, N. S.; Titta, A. D.; Piccapietra, F.; Dobias, J.; Nesatyy, V. J.; Suter, M. J. F.; Bernier-Latmani, R. Binding of silver nanoparticles to bacterial proteins depends on surface modifications and inhibits enzymatic activity. *Environ. Sci. Technol.* **2010**, *44* (6), 2163−2168, DOI: 10.1021/es903187s.
(30) Gao, J.; Youn, S.; Hovsepyan, A.; Llaneza, V. L.; Wang, Y.; Bitton, G.; Bonzongo, J. C. J. Dispersion and toxicity of selected manufactured nanomaterials in natural river water samples: Effects of water chemical composition. *Environ. Sci. Technol.* **2009**, *43* (9), 3322−3328, DOI: 10.1021/es803315v.
(31) Baalousha, M.; Nur, Y.; Römer, I.; Tejamaya, M.; Lead, J. R. Effect of monovalent and divalent cations, anions and fulvic acid on aggregation of citrate-coated silver nanoparticles. *Sci. Tot. Environ.* **2013**, *454*−*455*, 119−131, DOI: 10.1016/j.scitotenv.2013.02.093.
(32) He, D.; Bligh, M.; Waite, T. D. Effects of aggregate structure on the dissolution kinetics of citrate-stabilized silver nanoparticles. *Environ. Sci. Technol.* **2013**, *47* (16), 9148−9156, DOI: 10.1021/es400391a.
(33) Lubello, C.; Gori, R.; Nicese, F. P.; Ferrini, F. Municipal-treated wastewater reuse for plant nurseries irrigation. *Water Res.* **2004**, *38* (12), 2939−2947, DOI: 10.1016/j.watres.2004.03.037.
(34) Klein-BenDavid, O.; Gvirtzman, H.; Katz, A. Geochemical identification of fresh water sources in brackish groundwater mixtures; the example of Lake Kinneret (Sea of Galilee), Israel. *Chem. Geol.* **2005**, *214* (1−2), 45−59, DOI: 10.1016/j.chemgeo.2004.08.025.
(35) Hadi, K. M. B. Evaluation of the suitability of groundwater quality for reverse osmosis desalination. *Desalination* **2002**, *142* (3), 209−219, DOI: 10.1016/S0011-9164(02)00202-3.
(36) Chen, S.; Kimura, K. Water soluble silver nanoparticles functionalized with thiolate. *Chem. Lett.* **1999**, *28* (11), 1169−1170, DOI: 10.1246/cl.1999.1169.
(37) Ralling, G.; Bodrug, S.; Linn, T. Growth rate-dependent regulation of RNA polymerase synthesis in *Escherichia coli*. *MGG, Mol. Gen. Genet.* **1985**, *201* (3), 379−386, DOI: 10.1007/BF00331327.
(38) Afrooz, A. R. M. N.; Khan, I. A.; Hussain, S. M.; Saleh, N. B. Mechanistic heteroaggregation of gold nanoparticles in a wide range of solution chemistries. *Environ. Sci. Technol.* **2013**, *47* (4), 1853−1860, DOI: 10.1021/es3032709.
(39) Khan, I. A.; Afrooz, A. R. M. N.; Flora, J. R. V; Schierz, P. A.; Ferguson, P. L.; Sabo-Attwood, T.; Saleh, N. B. Chirality affects aggregation kinetics of single-walled carbon nanotubes. *Environ. Sci. Technol.* **2013**, *47* (4), 1844−1852, DOI: 10.1021/es3030337.
(40) Koressaar, T.; Remm, M. Enhancements and modifications of primer design program Primer3. *Bioinformatics* **2007**, *23* (10), 1289−1291, DOI: 10.1093/bioinformatics/btm091.
(41) Linnert, T.; Mulvaney, P.; Henglein, A. Surface chemistry of colloidal silver: Surface plasmon damping by chemisorbed iodide, hydrosulfide (SH-), and phenylthiolate. *J. Phys. Chem.* **1993**, *97* (3), 679−682, DOI: 10.1021/j100105a024.
(42) Mock, J. J.; Smith, D. R.; Schultz, S. Local refractive index dependence of plasmon resonance spectra from individual nanoparticles. *Nano Lett.* **2003**, *3* (4), 485−491, DOI: 10.1021/nl0340475.
(43) Mock, J. J.; Barbic, M.; Smith, D. R.; Schultz, D. A.; Schultz, S. Shape effects in plasmon resonance of individual colloidal silver nanoparticles. *J. Chem. Phys.* **2002**, *116* (15), 6755−6760, DOI: 10.1063/1.1462610.
(44) Willets, K. A.; Van Duyne, R. P. Localized surface plasmon resonance spectroscopy and sensing. *Annu. Rev. Phys. Chem.* **2007**, *58*, 267−297, DOI: 10.1146/annurev.physchem.58.032806.104607.
(45) Li, X.; Lenhart, J. J.; Walker, H. W. Aggregation kinetics and dissolution of coated silver nanoparticles. *Langmuir* **2012**, *28* (2), 1095−1104, DOI: 10.1021/la202328n.
(46) Mulvaney, P.; Linnert, T.; Henglein, A. Surface chemistry of colloidal silver in aqueous solution: Observations on chemisorption and reactivity. *J. Phys. Chem.* **1991**, *95*, 7843−7846, DOI: 10.1021/j100173a053.
(47) Kapoor, S. Preparation, characterization, and surface modification of silver particles. *Langmuir* **1998**, *14* (5), 1021−1025, DOI: 10.1021/la9705827.

(48) Ratte, H. T. Bioaccumulation and toxicity of silver compounds: A review. *Environ. Toxicol. Chem.* **1999**, *18* (1), 89−108, DOI: 10.1002/etc.5620180112.
(49) Jung, W. K.; Koo, H. C.; Kim, K. W.; Shin, S.; Kim, S. H.; Park, Y. H. Antibacterial activity and mechanism of action of the silver ion in *Staphylococcus aureus* and *Escherichia coli*. *Appl. Environ. Microbiol.* **2008**, *74* (7), 2171−2178, DOI: 10.1128/AEM.02001-07.
(50) Schellhorn, H. Regulation of hydroperoxidase (catalase) expression in *Escherichia coli*. *FEMS Microbiol. Lett.* **1995**, *131* (2), 113−119, DOI: 10.1111/j.1574-6968.1995.tb07764.x.
(51) Loewen, P. C.; Switala, J.; Triggs-Raine, B. L. Catalases HPI and HPII in *Escherichia coli* are induced independently. *Arch. Biochem. Biophys.* **1985**, *243* (1), 144−149, DOI: 10.1016/0003-9861(85)90782-9.
(52) Rudd, K. E. EcoGene: A genome sequence database for *Escherichia coli* K-12. *Nucleic Acids Res.* **2000**, *28* (1), 60−64, DOI: 10.1093/nar/28.1.60.
(53) Hwang, E. T.; Lee, J. H.; Chae, Y. J.; Kim, Y. S.; Kim, B. C.; Sang, B. I.; Gu, M. B. Analysis of the toxic mode of action of silver nanoparticles using stress-specific bioluminescent bacteria. *Small* **2008**, *4* (6), 746−750, DOI: 10.1002/smll.200700954.
(54) Choi, O.; Hu, Z. Size dependent and reactive oxygen species related nanosilver toxicity to nitrifying bacteria. *Environ. Sci. Technol.* **2008**, *42* (12), 4583−4588, DOI: 10.1021/es703238h.
(55) Park, H. J.; Kim, J. Y.; Kim, J.; Lee, J. H.; Hahn, J. S.; Gu, M. B.; Yoon, J. Silver-ion-mediated reactive oxygen species generation affecting bactericidal activity. *Water Res.* **2009**, *43* (4), 1027−1032, DOI: 10.1016/j.watres.2008.12.002.